Palladium–lanthanum interaction phenomena in Pd–$LaCl_3$/SiO_2 and Pd–La_2O_3/SiO_2 catalysts

X.L. Seoane [a,*], N.S. Fígoli [b], P.C. L'Argentiere [b], J.A. González [a] and A. Arcoya [a]

[a] *Instituto de Catálisis y Petroleoquímica, CSIC, Campus Universidad Autónoma, Cantoblanco, 28049 Madrid, Spain*
E-mail: JLSeoane@icp.csic.es
[b] *Instituto de Investigaciones en Catálisis y Petroquímica, INCAPE (UNL, FIQ-CONICET), Santiago del Estero 2654, 3000 Santa Fe, Argentina*

Received 27 February 1997; accepted 12 July 1997

The effect of La addition and the nature of the precursors on the surface properties of Pd/SiO_2 are studied. Samples containing 0.5 wt% Pd were prepared by incipient wetness impregnation and characterized by H_2 and CO chemisorption, TEM, TPR, EDX, XPS, Ar^+-sputtering and CO/FTIR. The use of nitrate precursors improves both reducibility and dispersion of Pd. Lanthanum addition makes the metal reduction more difficult, indicating that a Pd–La interaction takes place. When starting from Cl^- precursors, Pd^{n+} species are formed at the surface, whereas only Pd^0 is found when nitrate precursors are used. The addition of $LaCl_3$ increases the Pd dispersion and hinders the formation of Pd^{n+} species through a dilution effect. In a sample prepared from $Pd(NO_3)_2$ + $La(NO_3)_3$, the La_2O_3 formed upon calcination originates a SMSI-like effect on the palladium. This effect is suggested by the strong reduction of the H_2 and CO chemisorption capacity of Pd in this sample, in spite of the fact that the dispersion of palladium calculated from TEM increases in the presence of La. From XPS results this SMSI state appears to be due to a physical decoration of Pd by La_2O_3 rather than to an electronic Pd–La_2O_3 interaction. The "decoration model" is further confirmed by the progressive increase of the Pd/La atomic ratio observed upon XPS/Ar^+-sputtering at different times the sample containing La. The hypotheses of both dilution and decoration effects caused by $LaCl_3$ and La_2O_3, respectively, are strengthened by the CO/FTIR results.

Keywords: Pd catalysts, electron-deficiency, decoration, TPR, TEM, XPS, Ar^+-sputtering, CO/FTIR

1. Introduction

Supported Pd catalysts are widely used in several important commercial reactions, including selective hydrogenation of unsaturated organic groups for fine chemicals [1], selective or total hydrogenation of highly unsaturated hydrocarbons or aromatics [1,2], pollution control [3] and methanol synthesis from $CO + H_2$ [4]. It was reported that the addition of La_2O_3 enhances the palladium activity and selectivity for this last reaction [5,6], in spite of the fact that La_2O_3 is inactive for this reaction. Recently, it was also found that the incorporation of $LaCl_3$ or La_2O_3 to Pd/SiO_2 catalysts increases their resistance towards the toxic effect of thiophene in the ethylbenzene hydrogenation [7].

Several hypotheses have been put forward to explain this remarkable effect of lanthana. For instance, the occurrence of palladium in a SMSI state, responsible for its high reactivity, caused by the decoration of the metal particles by patches of LaO_x [8]. In this case, a transfer of the excess charge of La to Pd particles in the Pd–LaO_x interface was found by XPS, giving a Pd acting more as an electron-donor than Pd^0 [9]. Therefore, this SMSI effect is electronic in nature. In other cases, however, this decoration phenomenon is caused by the redissolution of the lanthana followed by its codeposition with the metal precursor during the impregnation step, without any charge transfer being detected in this process [10]. It has been also reported that the metal decoration/encapsulation can be related to the chemical and structural modifications undergone by La_2O_3 during the preparation of the catalyst [11,12]. Most of these works concern the effect of La_2O_3, those dealing with the effect of $LaCl_3$ being more scarce.

The present work is devoted to study the role of $LaCl_3$ and La_2O_3 on the reducibility, metal dispersion and surface chemical state of palladium in Pd/SiO_2 catalysts prepared from $PdCl_2$ and $Pd(NO_3)_2$, respectively. For that purpose, the samples with and without lanthanum were characterized by TPR, H_2 and CO chemisorption, TEM, XPS, Ar^+-sputtering and FTIR of adsorbed CO.

The occurrence of two different types of Pd–La interaction, namely dilution effect and decoration/encapsulation phenomena, depending on the chemical nature of the precursor salts used to prepare the samples, is discussed.

* To whom correspondence should be addressed.

2. Experimental

2.1. Preparation of the samples

Five samples containing 0.5 wt% Pd were prepared by the incipient wetness impregnation technique. Silica G-57 from W.R. Grace ($SiO_2 > 99.6\%$, BET surface area 300 $m^2\ g^{-1}$, pore volume 1 $cm^3\ g^{-1}$ and particle size 0.8–1.41 mm) was used as the support. It was previously calcined at 823 K. For samples NPdSi and CPdSi, acidic aqueous solutions of $Pd(NO_3)_2{\cdot}6H_2O$ (Sigma, $> 99.9\%$), and $PdCl_2$ (Sigma, $> 99.9\%$), respectively, were used. Samples NPdLaSi and CPdLaSi (La/Pd atomic ratio = 2) were prepared by coimpregnation of the silica with a solution containing either $Pd(NO_3)_2 + La(NO_3)_3{\cdot}6H_2O$ (Fluka, Puriss. p.a.) or $PdCl_2 + LaCl_3{\cdot}nH_2O$ (Fluka puriss. p.a.), respectively. The sample NPdLa was prepared by impregnation of La_2O_3 (Fluka, 99.9%) with a $Pd(NO_3)_2$ solution. The La_2O_3 was previously calcined at 773 K. After drying at 393 K overnight, precursors were calcined at 573 K for 4 h in flowing air (Air Liquid, 99.999%) and later reduced at 573 K for 5 h in a hydrogen stream (Air Liquid, 99.995%). Finally, the sample NLaSi, containing 3 wt% of La_2O_3 on SiO_2, was prepared by impregnating the support with $La(NO_3)_3$ solution, followed by calcination at 573 K in air and heating at the same temperature in a hydrogen stream. All the samples were kept in a desiccator before use. Chemical composition of the catalysts determined by atomic absorption spectroscopy practically corresponds to the nominal composition given in table 1. The La-species present on CPdLaSi is essentially $LaCl_3$. In fact, we have previously verified by XRD and XPS [7] that $LaCl_3$ calcined at 573 K is not transformed into LaOCl nor La_2O_3. LaOCl is only formed after calcination of $LaCl_3$ at 773 K, and La_2O_3 is not formed even after calcination at 1073 K.

2.2. Characterization of the samples

Reducibility of the calcined precursors of the samples was determined by temperature-programmed reduction (TPR) in a flow system with a thermal conductivity detector. Samples of 0.5 g were outgassed at 573 K for 1 h in an Ar stream (Air Liquid, 99.9995%) and then cooled to 273 K. TPR profiles were registered by heating the samples from 273 to 773 K, at 6 K min^{-1}, in a gas flow rate of 5% H_2/Ar (30 ml min^{-1}).

Table 1
Chemical composition of the samples

Sample	Precursors	Pd (wt%)	La (wt%)	La : Pd (atomic ratio)
NPdSi	$Pd(NO_3)_2{\cdot}6H_2O$	0.5	–	0
CPdSi	H_2PdCl_4	0.5	–	0
NPdLaSi	$Pd(NO_3)_2{\cdot}6H_2O$ $La(NO_3)_3{\cdot}nH_2O$	0.5	1.3	2
CPdLaSi	H_2PdCl_4 $LaCl_3{\cdot}nH_2O$	0.5	1.3	2
NPdLa	$Pd(NO_3)_3{\cdot}6H_2O$ La_2O_3 [a]	0.5	85.4	170
NLaSi	$La(NO_3)_3{\cdot}6H_2O$	–	2.6	–

[a] As support.

Dispersion (D) and *mean particle size* ($\bar{d}$) of Pd in the samples were measured by different techniques.

(i) Hydrogen chemisorption, by the hydrogen backsorption method using a volumetric adsorption system at room temperature, following the procedure previously described [7]. To calculate the number of surface palladium atoms (Pd_s) a H_{ads}/Pd_s stoichiometry = 1/1 was used.

(ii) Carbon monoxide chemisorption, by the pulse chromatographic method, using a Micromeritics Chemisorb 2700. Reduced samples of 0.3 g were outgassed at 573 K under a helium flow for 30 min. After cooling to RT, pulses of 50 μl of purified CO (Air Liquid, 99.97%) were injected in the helium carrier gas (Air Liquid, 99.999%) until saturation of the metal surface, which corresponds to irreversible chemisorption. A stoichiometry $Pd_s/CO_{ads} = 1.15/1$, as recommended by Farrauto [13], was used.

Using the values of Pd_s the metal dispersion in each sample was calculated by the expression

$$D(\%) = (Pd_s/Pd_t) \times 100\,, \tag{1}$$

where Pd_t is the total number of palladium atoms in the sample. When the metal surface is clean (no chemical species cover the surface) gas chemisorption gives the real dispersion values and these values are, therefore, comparable to those obtained by other methods.

From the dispersion values measured by CO chemisorption and assuming a spherical model for the palladium particle, the average particle size (diameter, $\bar{d}$) was calculated by

$$\bar{d} = \frac{105.5}{D(\%)}\ (\text{nm})\,. \tag{2}$$

(iii) Transmission electron microscopy (TEM), in a Jeol 100CX electron microscope, with 0.3 nm resolution. The operating voltage was 100 kV. The samples were examined at a magnification of 100 000X–140 000X.

The reduced powder was suspended in ketone and agitated in an ultrasonic bath for 5 min; a drop of the fine suspension was placed on a carbon-coated copper grid of 200 mesh, which was then loaded into the microscope. The surface mean particle diameter ($\bar{d}_s$) was calculated from the particle size distribution, according to the expression

$$\bar{d}_s = \frac{\sum n_i d_i^3}{\sum n_i d_i^2}\,, \tag{3}$$

where n_i is the number of particles having a diameter d_i.

An average of 400 particles were counted for each sample.

The energy-dispersive X-ray (EDX) analyses were carried out in a silicon–lithium diode detector (Link, model AN 1000).

Sample surface was analyzed by X-ray photoelectron spectroscopy (XPS) with a Shimadzu ESCA 750 electron spectrometer. The chemical state of Pd and La was characterized from the values of the binding energies (BE) of the maxima of the Pd $3d_{5/2}$ and La $3d_{5/2}$ peaks. Correction for binding energies due to sample charging was effected by taking the Si $2p_{1/2}$ line at 103.2 eV as an internal standard. After reduction, the samples were introduced into the sample holder under isooctane and protected from exposure to air by a meniscus of this liquid. Isooctane was removed during pumping in the preparation chamber of the XPS equipment. This operating procedure ensures that there is no modification of the chemical state of palladium, which is fairly stable [7].

Surface atomic ratios La/Pd, La/Si and Pd/Si were evaluated from the intensities of the peaks, using the equation

$$\frac{n_i}{n_j} = \frac{I_i/S_i}{I_j/S_j}, \qquad (4)$$

where n_i/n_j is the atomic ratio between the i and j species, I_i and I_j are the intensities of the corresponding peaks for the i and j atoms, and S is the atomic sensitivity factor: $S_{pd} = 4.6$ (3d level), $S_{La} = 10.0$ (3d level) and $S_{Si} = 0.27$ (2p level), given by Wagner et al. [14].

The spectrometer is equipped with Ar-etching facilities in the preparation chamber. An Ar^+ ion gun was used for different periods of time to remove the external layers of the surface. The residual gas pressure was 5×10^{-4} Pa and the beam voltage 2 kV. The Ar^+ ion beam was directed onto the sample and the irradiated spot was 0.8 cm^2.

The electronic state of palladium in the samples was studied by FTIR spectroscopy. The infrared spectra were recorded on a Nicolet 5ZDX FTIR spectrometer with a resolution of 4 cm^{-1}. The self-supported wafer of reduced catalyst (25 mg cm^{-2}) was outgassed in situ at room temperature for 1 h and then reduced again at 373 K under 10^4 Pa of hydrogen for 1 h. The sample was successively evacuated at 2×10^{-2} Pa at this temperature for 30 min and cooled at room temperature. After recording the background spectrum at room temperature, the sample was contacted with 2×10^3 Pa of CO for 10 min and them the new spectrum registered. The IR spectrum of the adsorbed CO was obtained by subtraction of both spectra. To improve the signal to noise ratio a scan number of 128 was chosen. The spectra range at 2200–1800 cm^{-1} was analyzed.

3. Results and discussion

3.1. TPR

TPR profiles of the samples prepared from chlorides (CPdSi and CPdLaSi) have been analyzed in detail in ref. [7], samples A and C, respectively. Briefly, they show a single H_2 uptake peak (figures 1a and 1b), corresponding to the total reduction of Pd^{2+} to Pd^0 ($H_2/Pd^{2+} \approx 1$). The addition of $LaCl_3$ retards the reducibility of the $PdCl_2$, as it is evidenced by the shift of the maximum of the peak from 367 to 393 K (see table 2).

As expected, the TPR profile of NPdSi does not show any reduction peak (figure 1c), because calcination of $Pd(NO_3)_2$ at 573 K leads to PdO, which is reduced at sub-ambient temperature [15]. This is evidenced by the negative peak recorded at 342 K, corresponding to the decomposition of the β-PdH formed upon absorption of hydrogen in Pd^0. In contrast, $PdCl_2$ calcined at 573 K remains as such compound, which is more difficult to reduce than PdO.

TPR of NPdLaSi displays a sharp peak of H_2 consumption at 343 K (figure 1d), which corresponds to the complete reduction $Pd^{2+} \rightarrow Pd^0$. This result proves that the presence of La_2O_3 on NPdLaSi retards the reduction of PdO and, therefore, that a Pd–La_2O_3 interaction exists. In addition, a broad peak is observed at ca. 623 K in figure 1d. This peak is not due to the reduction of lanthana, because we have verified by TPR that neither commercial lanthana nor La_2O_3/SiO_2 exhibit any H_2 uptake. Furthermore, when reduced NPdLaSi was recalcined in air at 773 K, a single peak corresponding to the reduction of Pd^{2+} is present (figure 1e). This result also proves that, under our conditions, La_2O_3 is not reduced even in the presence of Pd. Then, it seems that this peak must rather be ascribed to the reduction and/or desorption of some residual adsorbed NO_x. Actually, a similar peak is observed in the TPR of lanthana impregnated with HNO_3, calcined at 573 K, but it is absent in the TPR of the reduced sample NPdLaSi. This means that during the reduction step at 573 K, when preparing the samples, the nitrogen species are completely eliminated.

The TPR profile of NPdLa (figure 1f) exhibits a Pd^{2+} reduction peak broader than that of NPdLaSi (figure 1d) and shifted to a higher temperature. This result indicates that the interaction Pd–La_2O_3 is stronger when lanthana is used as a support than when it is used as an additive.

3.2. Dispersion

From the H_2 and CO chemisorption data, dispersion of Pd in sample NPdSi is higher than in CPdSi (table 2). These data also show that lanthanum provokes opposite effects on the metal dispersion when measured by gas chemisorption, depending on the chemical nature of the Pd and La precursors. Thus, for the sample prepared from chlorides (CPdLaSi), lanthanum increases the gas

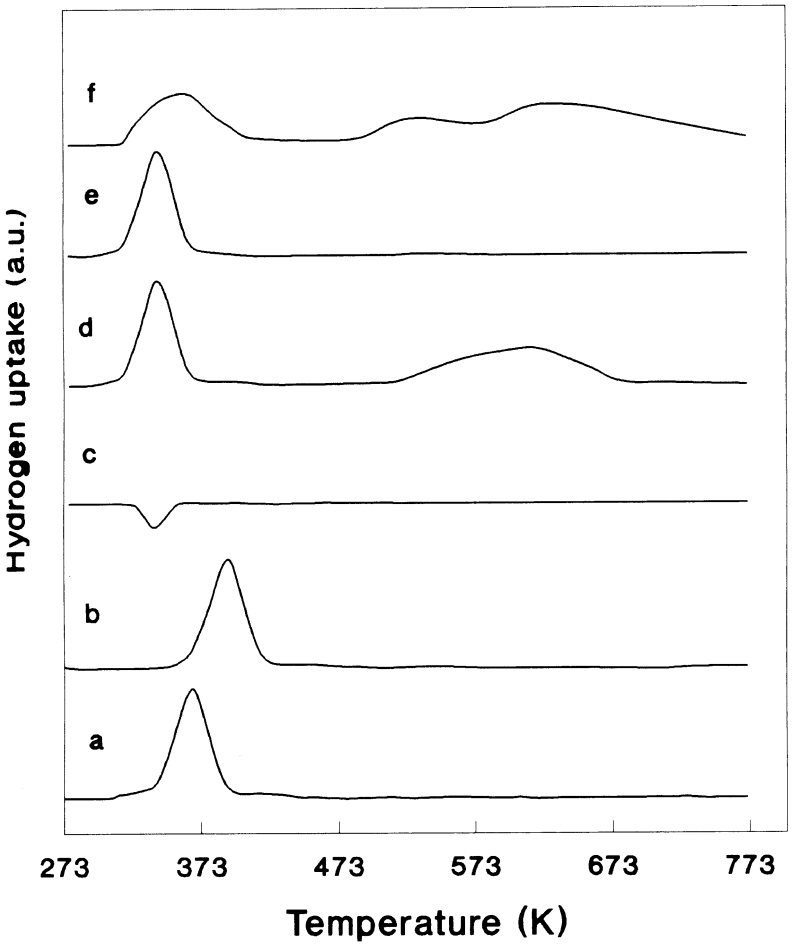

Figure 1. TPR profiles of the samples: (a) CPdSi; (b) CPdLaSi; (c) NPdSi; (d) NPdLaSi; (e) NPdLaSi reoxidized in air at 773 K and (f) NPdLa.

chemisorption capacity and, therefore, the dispersion of palladium, as it is calculated from H_2 or from CO adsorption. In contrast, for the sample prepared from nitrates (NPdLaSi), the presence of lanthanum produces a strong decrease of both H_{ads} and CO_{ads}. Similar low dispersion values were found for the NPdLa sample (table 2).

Micrographs of NPdLaSi obtained by TEM show a moderate contrast between lanthanum compounds and palladium particles, which were identified by EDX. A micrograph in which the metal particles can be clearly visualized is shown in figure 2. The average particle size of palladium calculated by eq. (3) is $\bar{d}_s \approx 3.0$ nm, from which the palladium dispersion was estimated to be about 35%, whereas the H_{ads}/Pd_t and CO_{ads}/Pd_t ratios give values about 3% ($\bar{d} \approx 35$ nm, table 2). Additionally, the EDX examination of this sample showed that the palladium particles are always located together with lanthanum compound particles. Analogous results were found for the sample NPdLa. For the NPdSi, the average particle size of palladium calculated by TEM (figure 3) is $\bar{d}_s \approx 6.2$ nm ($D \approx 17\%$), in agreement with the values obtained from gas chemisorption.

Table 2
Characterization of the samples by TPR, gas chemisorption and TEM

Sample	TPR T_{max} (K)	D (%) H_2	D (%) CO	$\bar{d}_s$ (nm) TEM	D (%) TEM
NPdSi	(342) [a]	15	17	6.2	17.1
CPdSi	367	12	11	–	–
NPdLaSi	343	3	4	3.0	35.3
CPdLaSi	393	20	18	–	–
NPdLa	363	3	3	–	–

[a] Negative peak.

As a consequence, our results indicate that whatever the Pd precursor is, the addition of La, either as $LaCl_3$ or $La(NO_3)_3$, produces a decrease of the palladium particle size, but significantly suppresses the gas chemisorption and "apparently" decreases the dispersion when nitrate is used as lanthanum precursor. These findings suggest the occurrence of a SMSI-like palladium–lanthana interaction in NPdLaSi and NPdLa, similar to that found by several authors for Pd–La_2O_3 systems [5,8,9].

3.3. XPS

XPS results (see table 3) also prove that surface properties of the reduced samples are modified in a different

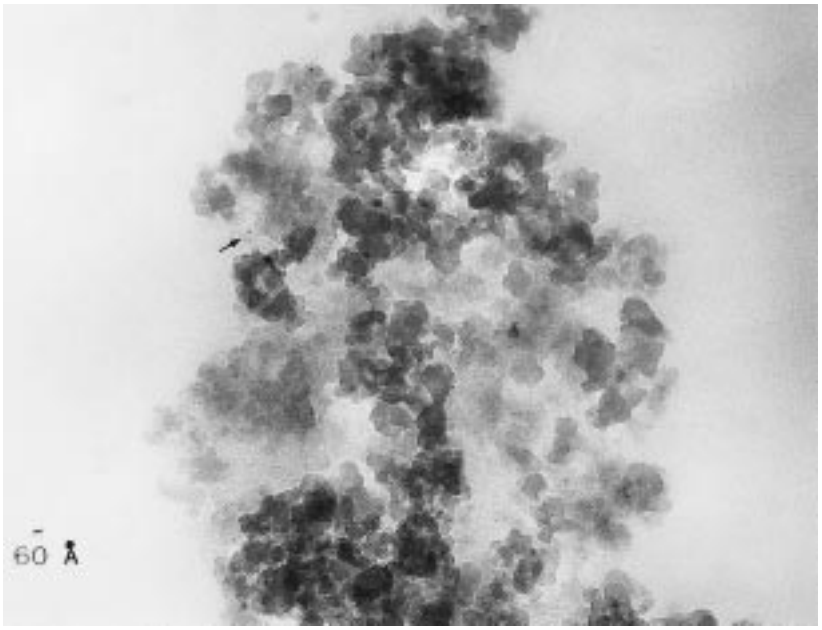

Figure 2. Micrograph of the sample NPdLaSi.

way by both the lanthanum addition and the nature of the precursor salts. Thus, while in the NPdSi sample Pd is found in metallic state (Pd^0, BE = 335.0 eV), in the surface of CPdSi partially oxidized Pd^{n+} species (BE = 336.5 eV and FWHM = 3.5 eV) are also formed, through the mechanism discussed in ref. [16]. On the other hand, we have also shown that the incorporation of $LaCl_3$ to a Pd/SiO_2 catalyst prepared from $PdCl_4H_2$ decreases the surface concentration of electron-deficient Pd^{n+} species (see table 3). To explain this effect it was proposed that, in this case, the $LaCl_3$ plays a diluent role, disrupting the palladium ensembles and hindering the formation of Pd^{n+} [7]. In sample NPdLaSi the BE values for Pd and La correspond to Pd^0 and La_2O_3, respectively (table 2). Thus, in contrast with that observed by other authors [9,17], in this sample no electron transfer La↔Pd was not detected by XPS.

In CPdSi and CPdLaSi, surface Pd/Si and La/Si atomic ratios calculated from XPS (table 3) suggest that in these samples both Pd and La are preferentially depos-

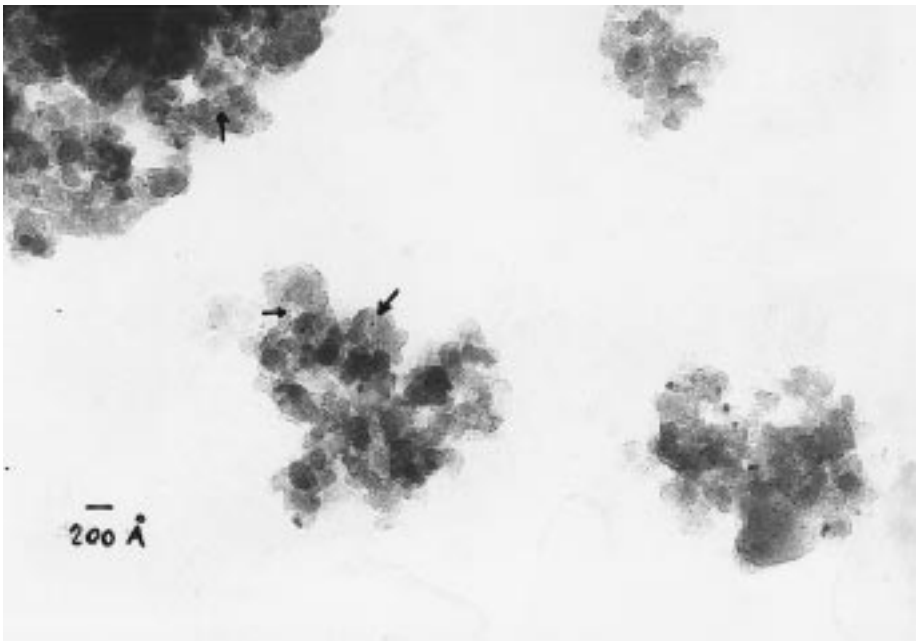

Figure 3. Micrograph of the sample NPdSi.

Table 3
XPS results

Sample	Pd $3d_{5/2}$ (eV)	FWHM (eV)	La $3d_{5/2}$ (eV)	Pd : Si		La : Si		La : Pd	
				bulk	XPS	bulk	XPS	bulk	XPS
Pd (foil)	335.1	–	–	–	–	–	–	–	–
Pd/SiO_2 [a]	335.2	2.3	–	–	–	–	–	–	–
La_2O_3 [b]	–	–	834.6	–	–	–	–	–	–
NLaSi	–	–	834.5	–	–	0.0111	–	–	–
NPdSi	335.0	2.1	–	0.0028	0.046	–	–	–	–
CPdSi	336.5	3.5	–	0.0028	0.038	–	–	–	–
NPdLaSi	335.1	2.1	834.5	0.0028	0.007	0.0056	0.06	2	9.1
CPdLaSi	335.8	2.8	833.6	0.0028	0.045	0.0056	0.07	2	1.6
NPdLa	335.2	2.2	834.4	–	–	–	–	127	10.3

[a] Prepared from $PdCl_2$. Reduced at 723 K (27). No Cl $2p_{3/2}$ peak is detected.
[b] This work.

ited at the outer surface of the support. A different result was obtained for samples prepared from nitrates. Thus, whilst the atomic ratio Pd/Si in NPdSi (table 3) indicates that most of the Pd is located at the outer surface of the silica particles, as in CPdSi, the low values of Pd/Si and Pd/La suggest that in NPdLaSi the surface of palladium is at least partially covered by La_2O_3. This fact would explain the low amounts of H_2 and CO chemisorbed on Pd in this sample and the EDX results, and it supports the existence of a Pd–La SMSI suggested above. The unreducibility of the lanthana together with the absence of any detectable charge transfer $Pd \leftrightarrow La_2O_3$, proves that this SMSI-effect is not electronic in nature, contrary to that found in other cases [9]. It seems that the particular behaviour of palladium in NPdLaSi, as well as in NPdLa, may rather be the consequence of the decoration/encapsulation of the Pd crystallites by La_2O_3 particles, which consists of the physical covering of the palladium particles by some lanthanum oxide, in a manner analogous to that described in ref. [18] for the Rh/TiO_2 system. This model has been frequently proposed in order to explain the SMSI effects observed in noble metal/oxide catalysts [12,19].

3.4. Sputtering

The decoration model is confirmed by the results obtained upon XPS/Ar^+-sputtering the samples CPdLaSi, NPdLaSi and NPdLa (see table 4). For samples NPdLaSi and NPdLa, the intensity of the La signal decreases progressively as the time of sputtering increases, indicating that sputtering by Ar^+ removes the thick La_2O_3 overlayer that could cover the palladium particles, thus inhibiting the H_2 and CO adsorption by the metal. In contrast, for sample CPdLaSi the La/Pd ratio remains constant and equal to the initial value after 10 min of sputtering.

Table 4
Results of XPS/Ar^+-sputtering

Time of sputtering (min)	La/Pd (atom/atom)		
	NPdLaSi	NPdLa	CPdLaSi
0	9.1	10.3	1.6
2	5.9	8.7	1.5
4	5.3	6.1	1.6
10	5.0	6.0	1.6

3.5. FTIR

The hypotheses of the diluent effect produced by La^{3+} in the sample CPdLaSi, and that of the decoration of Pd by La_2O_3 in samples NPdLaSi and NPdLa, are both strengthened by the FTIR results (figure 4). The IR spectrum of CO adsorbed on sample CPdSi shows three bands at ca. 1948, 2090 and 2135 cm^{-1}, respectively. The broad band at 1948 cm^{-1} is constituted by several superimposed bands, which are characteristic of different forms of bridged carbonyls on palladium [20,21]. The band at 2090 cm^{-1}, with a shoulder at 2045 cm^{-1}, corresponds to linearly bound CO on Pd^0 surface sites. Finally, the band at 2135 cm^{-1} is attributed to a linear CO bonded to palladium atoms having a lower electron density than Pd^0 [22], which confirms the existence of electron-deficient Pd^{n+} species on this reduced sample, as it was evidenced by the XPS results.

In comparison with the CPdSi sample, the spectrum of CPdLaSi shows a narrower and less intense band of bridged CO, which is shifted to a higher wavenumber (ca. 1958 cm^{-1}), indicating that a strong decrease in the number of bridged carbonyl species on surface palladium crystals occurs. This is the expected result if one accepts that, in this sample, $LaCl_3$ produces a diluent effect on the surface palladium. On the other hand, in the region of the linearly bonded CO, the band at 2135 cm^{-1} is absent, while the band corresponding to the CO–Pd^0 bond increases and slightly shifts to higher CO stretching frequencies. This behaviour, produced by the presence of $LaCl_3$, is consistent with both the decrease of Pd^{n+}

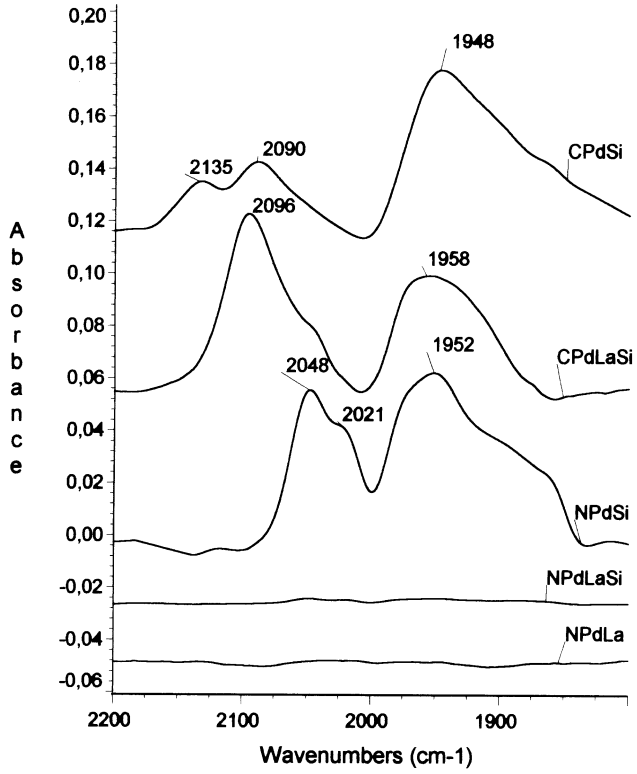

Figure 4. Infrared spectra of carbon monoxide adsorbed on the samples at RT.

concentration and the increase of the palladium capacity to chemisorb CO.

The CO adsorbed on NPdSi produces a band at ca. 2048 cm^{-1} with a shoulder at ca. 2021 cm^{-1} (figure 4), which is located in the range characteristic of linear CO–Pd^0 bond [23,24]. Furthermore, the broad band corresponding to CO bridging (ca. 1952 cm^{-1}) is also observed. As expected for this sample, no frequency related to electron-deficient palladium is detected. Finally, the IR spectra of NPdLaSi and NPdLa do not display any significant CO adsorption bands, providing additional evidence of the decoration model proposed above for these two samples.

From our point of view, the above results reasonably favour the idea that the different effects produced by lanthanum can be related to the different lanthanum compound present in each sample. Thus, in the sample CPdLaSi, lanthanum is found as $LaCl_3$ [7], which is already present in the impregnation solution all-together with the $PdCl_2$ and does not experience any chemical change during the calcination step at 573 K. For this reason, after reduction, Pd and $LaCl_3$ particles remain in the close vicinity of each other on the surface of the sample, allowing the $LaCl_3$ to play a diluent role. In contrast, in NPdLaSi and NPdLa lanthanum is found as La_2O_3, which is formed during the calcination of the sample by chemical decomposition of the $La(NO_3)_3$ incorporated to the impregnating solution. During this step, the palladium nitrate is also transformed into PdO, which is further reduced to metallic Pd. In this case, it seems very feasible that a consequence of these chemical processes may be the decoration/encapsulation of palladium crystallites by lanthana.

4. Conclusions

Samples prepared from nitrate precursors are easier to reduce than those prepared from chloride precursors. In these latter samples, after complete reduction, in addition to Pd^0, electron-deficient Pd^{n+} species are also observed by XPS and FTIR, whereas in the samples derived from nitrates only Pd^0 is found. For samples containing lanthanum, the palladium reduction peaks in TPR profiles shift to higher temperatures, indicating that a Pd–La interaction is taking place. $LaCl_3$ addition to Pd/SiO_2 increases the Pd dispersion and decreases its BE. The $LaCl_3$ produces a diluent effect on the surface palladium, a proposal supported by the relative decrease of the CO–Pd bridged bands observed by FTIR.

In the sample prepared by coimpregnation of silica with a solution containing $Pd(NO_3)_2$ and $La(NO_3)_3$, the La_2O_3 formed upon calcination originates an SMSI-like effect on Pd, without any electron transfer Pd–La_2O_3 being detected by XPS. This SMSI effect is suggested by the strong decrease of the H_{ads} and CO_{ads} values, and the fact that the crystal size of palladium calculated by TEM is smaller when the sample contains La_2O_3. The significant decrease of the Pd/Si and Pd/La atomic ratios, calculated by XPS, the XPS/Ar^+-sputtering results, and the FTIR spectra support, in this case, the proposal that the surface of palladium is decorated or encapsulated by lanthana particles.

Acknowledgement

Financial support from CICYT, Spain (Project MAT95-0783), CONICET, Argentina (Project ID 640), and the Programa de Cooperación Científica con Iberoamérica of the MEC (ICI-AECI), Spain, is gratefully acknowledged.

References

[1] *The Catalytic Reaction Guide* (Johnson Matthey, Royston, 1988).
[2] Z. Karpinski, Adv. Catal. 37 (1990) 45.
[3] H. Muraki, H. Shinjoh and Y. Fujitani, Appl. Catal. 22 (1986) 325.
[4] K.P. Kelly, T. Tatsumi, T. Uematsu, D.J. Driscoll and J.H. Lunsford, J. Catal. 101 (1986) 396.
[5] Ch. Sudhakar and M.A. Vannice, J. Catal. 95 (1985) 227.
[6] Yu.N. Nogin, N.V. Chesnokov and V.I. Kovalchuk, Catal. Lett. 23 (1994) 79.

[7] N.S. Fígoli, P.C. L'Argentiere, A. Arcoya and X.L. Seoane, J. Catal. 155 (1995) 95.
[8] J.S. Rieck and A.T. Bell, J. Catal. 96 (1985) 88.
[9] T.H. Fleisch, R.F. Hicks and A.T. Bell, J. Catal. 87 (1984) 398.
[10] R. Kieffer, A. Kiennemann, M. Rodriguez, S. Bernal and J.M. Rodriguez-Izquierdo, Appl. Catal. 42 (1988) 77.
[11] C. Sudhakar and M.A. Vannice, Appl. Catal. 14 (1985) 47.
[12] S. Bernal, F.J. Botana, R. Garcia and J.M. Rodriguez-Izquierdo, Stud. Surf. Sci. Catal. 48 (1989) 123.
[13] J.R. Farrauto, AIChE Symp. Ser. 70 (1974) 143.
[14] C.D. Wagner, L.E. Davis, M.V. Zeller, J.A. Taylor, R.H. Raymond and L.H. Gale, Surf. Interf. Anal. 3 (1981) 211.
[15] N.W. Hurst, S.J. Gentry, A. Jones and B.D. MacNicol, Catal. Rev. Sci. Eng. 24 (1982) 233.
[16] X.L. Seoane, P.C. L'Argentiere, N.S. Fígoli and A. Arcoya, Catal. Lett. 16 (1992) 137.
[17] J.M. Driessen, E.K. Poels, J.P. Hindermann and V. Ponec, J. Catal. 82 (1983) 26.
[18] R. Burch, in: *Hydrogen Effect in Catalysis*, eds. Z. Paál and P.D. Menon (Dekker, New York, 1988) p. 366.
[19] A.R. González-Elipe, P. Malet, J.P. Espinos, A. Caballero and G. Munuera, Stud. Surf. Sci. Catal. 48 (1989) 427.
[20] F. Pinna, M. Selva, M. Signoretto, G. Strukul, F. Boccuzzi, A. Benedetti, P. Canton and G. Fagherazzi, J. Catal. 150 (1994) 356.
[21] P. Marécot, A. Akhachane and J. Barbier, Catal. Lett. 36 (1996) 37.
[22] W. Juszkyk, Z. Karpinski, I. Ratajczykowa, Z. Stanasiuk, J. Zielinski, L.L. Sheu and W.M.H. Sachtler, J. Catal. 120 (1989) 68.
[23] M.A. Vannice, S.Y. Wang and S.H. Moon, J. Catal. 71 (1981) 152.
[24] L.M. Kustov, D. Osgard and W.M.H. Sachtler, Catal. Lett. 9 (1991) 121.